

## TEST OF FRAGMENTATION MODELS BY COMPARISON WITH THREE-JET EVENTS PRODUCED IN $e^+e^- \rightarrow$ HADRONS

JADE Collaboration

U. BARTEL, L. BECKER, C. BOWDERY<sup>1</sup>, D. CORDS, R. EICHLER<sup>2</sup>, R. FELST, D. HAIDT,  
H. KREHBIEL, B. NAROSKA, J. OLSSON, P. STEFFEN, P. WARMING  
*Deutsches Elektronen-Synchrotron DESY, Hamburg, Germany*

G. DIETRICH, E. ELSEN<sup>3</sup>, G. HEINZELMANN, H. KADO, K. MEIER, A. PETERSEN,  
U. SCHNEEKLOTH, G. WEBER  
*II. Institut für Experimentalphysik, Universität Hamburg, Germany*

S. BETHKE, A. DIECKMANN, J. HEINTZE, K.H. HELLENBRAND, R.D. HEUER, S. KOMAMIYA,  
J. von KROGH, P. LENNERT, H. MATSUMURA, H. RIESEBERG, J. SPITZER, A. WAGNER<sup>4</sup>  
*Physikalisches Institut der Universität Heidelberg, Germany*

A. BELL<sup>5</sup>, A. FINCH, F. FOSTER, G. HUGHES, T. NOZAKI, H. WRIEDT  
*University of Manchester, England*

J. ALLISON, J. BAINES, A.H. BALL, R.J. BARLOW, J. CHRIN, I.P. DUERDOTH, I. GLENDINNING,  
F.K. LOEBINGER, A.A. MACBETH, H. McCANN, H.E. MILLS, P.G. MURPHY, P.G. ROWE, K. STEPHENS  
*University of Manchester, England*

D. CLARKE, R. MARSHALL, G.F. PEARCE, J.B. WHITTAKER  
*Rutherford Appleton Laboratories, Chilton, England*

and

J. KANZAKI, T. KAWAMOTO, T. KOBAYASHI, M. KOSHIBA, M. MINOWA, M. NOZAKI, S. ODAKA,  
S. ORITO, A. SATO, H. TAKEDA, T. TAKESHITA, Y. TOTSUKA and S. YAMADA  
*Laboratory of International Collaboration on Elementary Particle Physics and Department of Physics,  
University of Tokyo, Japan*

Received 9 September 1983

The energy flow and particle flow distributions of planar three-jet events produced in  $e^+e^- \rightarrow$  hadrons at CM energies between 29.5 and 36.4 GeV have been interpreted in terms of the reaction  $e^+e^- \rightarrow q\bar{q}g$  and compared with the distributions calculated from two different fragmentation schemes, one based on independent parton fragmentation, the other one on fragmentation along colour flux lines. The particle density at angles between the two highest energy jets is found to decrease more strongly with increasing transverse mass of the particles than the particle density at angles between any of these jets and the lowest energy jet. The high momentum particles within the two most energetic jets are emitted at larger angles with respect to the lowest energy jet than the average particles. These observations are well reproduced by fragmentation along colour flux lines, but not by independent parton fragmentation.

<sup>1</sup> European Science Exchange Fellow.

<sup>2</sup> Now at Labor für Hochenergiephysik der ETH-Zürich,  
Villigen, Switzerland.

<sup>3</sup> Now at SLAC, CA, USA.

<sup>4</sup> Heisenberg Foundation Fellow.

<sup>5</sup> Now at British Petroleum, London, England.

We report on the comparison of three-jet events observed in  $e^+e^- \rightarrow$  hadrons with different fragmentation schemes, based on the interpretation of these jets as the debris of gluons and quarks produced in the gluon bremsstrahlung process  $e^+e^- \rightarrow q\bar{q}g$ . The energy and angular distributions of three-jet events do indeed support this interpretation [1], as does the observation of four-jet structures due to higher order diagrams [2]. However, in all these processes the parton dynamics (QCD) must be deciphered from the final state hadron distributions, a procedure which necessarily involves the fragmentation as an intermediate step. A precise understanding of fragmentation must therefore precede any quantitative test of QCD.

The present analysis is based on 18 424 multi-hadron events produced at CM energies between 29.5 and 36.4 GeV at the  $e^+e^-$  storage ring PETRA and recorded by the JADE detector. The detector, the trigger conditions and the selection of events are described in previous publications [3,4]. Events are classified according to their configuration in momentum space using the eigenvalues  $Q_1, Q_2,$  and  $Q_3$  of the normalized sphericity tensor ( $Q_1 < Q_2 < Q_3; Q_1 + Q_2 + Q_3 = 1$ ) and the related unit vectors  $\mathbf{q}_1, \mathbf{q}_2, \mathbf{q}_3$  of the principal axes. Planar events are selected by requiring  $Q_1 < 0.06$  and  $Q_2 - Q_1 > 0.07$ . Three jets of particles are defined by maximizing the triplicity [5]. Jet direction  $\mathbf{k}_j$  is given by the vector sum of the particle momenta within jet  $j$ . The three jets are projected on to the event plane defined by  $(\mathbf{q}_2, \mathbf{q}_3)$  and ordered such that jet #1 is opposite the smallest angle, and jet #3 opposite the largest angle between the jet directions. Events with jets containing less than 4 particles, or with jet energy less than 2 GeV, are rejected. After these cuts we are left with 2048 planar three-jet events.

In order to investigate how the different fragmentation schemes manifest themselves in the final state hadron distribution extensive model calculations were performed. In these calculations the partons from the reaction  $e^+e^- \rightarrow q\bar{q}g$  were created according to the first-order QCD with a quark-gluon coupling strength  $\alpha_2 = 12\pi/23 \ln(s/\Lambda^2)$  and  $\Lambda = 0.3$  GeV. The analysis, however, is rather independent of the  $\alpha_s$  value chosen. Increasing for instance in the Lund model  $\Lambda$  to 1.5 GeV, one reduces the background from  $q\bar{q}$ -events in the three-jet sample from 14% to 10% and all model results quoted remain the same as for  $\Lambda = 0.3$  within the statistical errors.

One of the fragmentation schemes studied assumes that the quark, antiquark and gluon of a three-jet event fragment independently of each other, as expected if jet evolution proceeds by branching processes down to small off-shell masses with non-perturbative long range effects playing a minor role [6,7]. For independent fragmentation of quarks and gluons the model of Hoyer et al. [7] was used. It assumes a gaussian distribution of the transverse momenta of secondary quarks relative to the primary quark direction  $d\sigma/dp_\perp^2 \sim \exp(-p_\perp^2/2\sigma_{q,q}^2)$  in the overall CM system and a fragmentation function for the longitudinal momentum distribution  $f(z) = 1 - a_q + 3a_q(1-z)^2$  for  $a_q < 1$ , and  $f(z) = (1+a_q)(1-z)^{a_q}$  for  $a_q > 2$ .  $a_q$  is an empirical parameter which depends e.g. on the quark mass. Gluons are treated as quark-antiquark pairs with the gluon momentum carried entirely by one of the quarks, which subsequently fragments with distributions parametrized by  $\sigma_{q,g}$  and  $a_g$ . As reported elsewhere [8], different gluon fragmentation parameters are needed to obtain a reasonable fit to the observed distributions. The following parameters were used: A production ratio of secondary u, d, and s quarks of 3 : 3 : 1, equal fraction of pseudoscalar and vector mesons,  $\sigma_{q,q} = 330$  MeV,  $\sigma_{q,g} = 500$  MeV, and  $a_q = 0.5$  for the light quarks,  $a_q = 0.0$  for the heavy ones, and  $a_g = 4.0$  for the gluon.

The second scheme is the Lund model [9], in which fragmentation proceeds along the colour flux lines. For  $q\bar{q}g$ -events, these flux lines connect the gluon with the quark and antiquark, but do not connect the quark and antiquark directly. For more details see ref. [9]. The parameters are the same as for quarks of the first scheme except for the fragmentation function which is replaced by  $f(z) = (1+\beta)(1-z)^\beta$  with  $\beta = 0.4$  for the light quarks and  $\beta = 0.1$  for heavier ones. The parametrization, however, is applied in the string rest system which is defined by the quark (or antiquark) plus half the gluon momentum. The parameters of both the model of Hoyer et al. and the Lund model have been adjusted to give a reasonable agreement with the data.

Monte Carlo techniques were used to calculate the four-momenta of the final state particles, including bremsstrahlung from the initial leptons. In a second step, the generated events were passed through a simulation of the detector with all known imperfections and were processed by the same chain of com-

puter programs and cuts as the real data. These model calculations show, almost independently of the assumed gluon fragmentation, that in about 50% of the cases jet #3 is created by the gluon.

In a previous letter [3] we have compared these two extreme models with the data and shown that the particle densities in the angular gaps between the jets are better reproduced by fragmentation along the colour-anticolour axes than by fragmentation along the parton directions. In the present paper, using a larger data sample than in the first report, we corroborate this evidence by studying the complete energy and particle flow distributions as well as the correlation of the transverse and longitudinal momentum components of the particles in a jet. In the previous [3] and in the present investigation, both charged and neutral particles were used for the event selection, the determination of the sphericity tensor and in the identification of jets and their directions. However, the particle distributions shown in figs. 1-3 are for charged particles only. Within the statistical errors they agree with the distributions obtained, when both charged and neutral particles are included [10].

Characteristic differences between the two fragmentation schemes become visible in the energy flow distribution of the events. These distributions are obtained by projecting all particle momenta of an event on to the  $(q_2, q_3)$ -plane and summing the particle energies in angular bins. An angle  $\theta$  is defined in the event plane between the particle momentum and the axis of jet #1, and runs via jets #2 and #3 back to #1. Thus the axis of jet #1 is fixed at  $0^\circ$ , whereas the axis of jets #2 and #3 are distributed around  $155^\circ$  and  $230^\circ$ , respectively. The differential energy flow is normalized to the total energy observed.

Fig. 1a shows a comparison of the experimental energy flow with the two model predictions. The relative differences between the two model calculations are largest in the region between jets #1 and #2 and the data are obviously better described by the Lund model. A comparison of the 14 data points in the region  $50^\circ < \theta < 120^\circ$  yields  $\chi^2 = 17$  for the Lund model and  $\chi^2 = 42$  for the model of Hoyer et al.. A comparison of the particle flow, with the model results in fig. 1b confirms this observation.

According to the Lund model, the observed depletion between jets #1 and #2 arises from the fragmentation proceeding in the coordinate subsystems of the

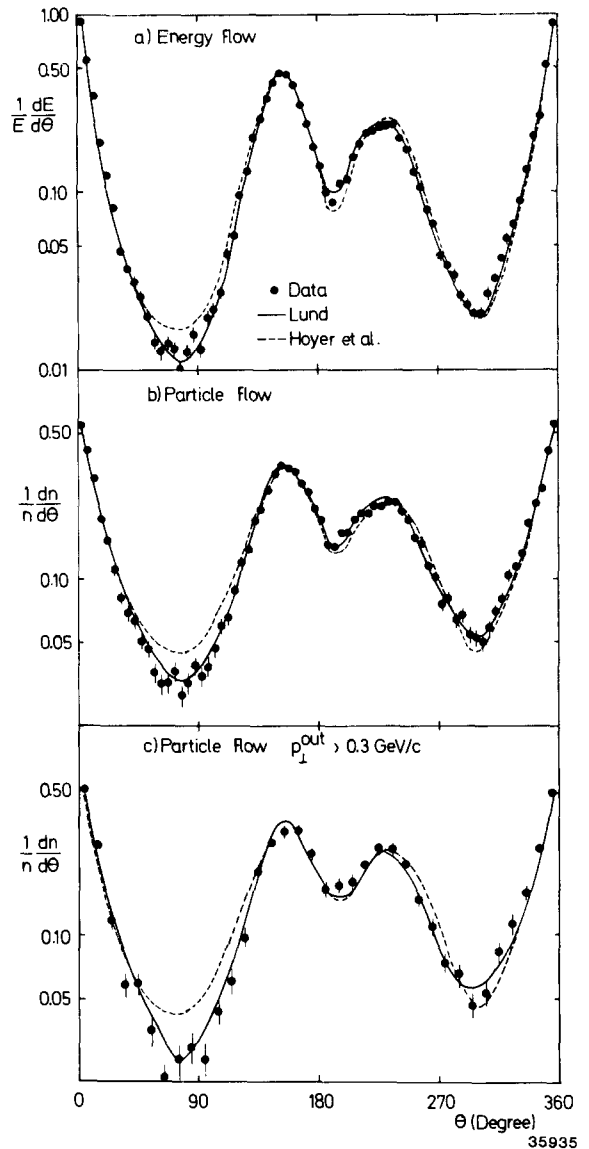


Fig. 1. (a) The normalized energy flow  $(1/E)dE/d\theta$  together with the model predictions. (b) The normalized charged particle flow  $(1/n)dn/d\theta$ . (c) The normalized charged particle flow  $(1/n)dn/d\theta$  for particles with  $p_{\perp}^{\text{out}} > 0.3 \text{ GeV}/c$ .  $n$  is the total number of particles used in each plot.

colour strings which to the observer in the overall CM system appears Lorentz-transformed towards the gluon hemisphere. For example, a particle with its momentum vector normal to the event plane ( $\mathbf{p} = \mathbf{p}_{\perp}^{\text{out}}$ ) in the colour string subsystem will acquire a momen-

tum component in the direction of the Lorentz boost given by  $\beta\gamma[m^2 + (p_{\perp}^{\text{out}})^2]^{1/2}$ , where  $\beta$  and  $\gamma$  are respectively the velocity and the Lorentz factor of the string subsystem relative to the overall CM system. Consequently, the differences between the two models ought to become more pronounced for particles with larger values of  $[m^2 + (p_{\perp}^{\text{out}})^2]^{1/2}$ . In fig. 1c, where the particle flow is plotted only for particles with  $p_{\perp}^{\text{out}} > 0.3 \text{ GeV}/c$ , the differences between the two models are indeed more pronounced, and again the Lund model provides a better description of the data.

Another way of revealing these differences is to plot the distributions such that the jet axes of all events coincide. This is achieved, by plotting the particle density as a function of the normalized projected angle  $\theta_{i,j}/\theta_{jk}$  where  $\theta_{jk}$  is the angle between the jet axes # $j$  and # $k$ , and  $\theta_{i,j}$  is the angle between jet axis # $j$  and the direction of the particle  $i$ , as sketched in the upper corner of fig. 2. The distribution is normalized to the total number of particles of the events. This density is shown in fig. 2. Both models describe the data well, except for the region between jets #1 and #2, where the model of Hoyer et al. predicts more particles than observed experimentally.

As a relative measure of the particle density in the region between the jets the ratio of the number of particles in the range  $0.3 < \theta_{i,j}/\theta_{jk} < 0.7$  between jets #1 and #3 to the number between jets #1 and #2 is taken. This ratio is listed in the first row of table 1, together with the model predictions. The observed behaviour persists, even if the lower momen-

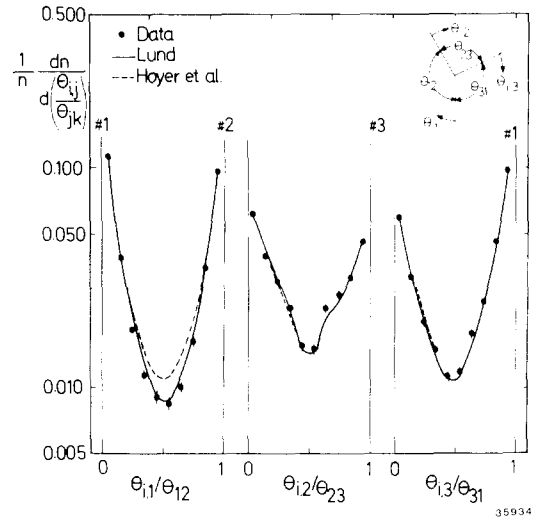


Fig. 2. The average charged particle density in the angular regions between the jet axes normalized to the total number of particles versus  $\theta_{i,j}/\theta_{jk}$ . The data are compared with the Hoyer et al. and Lund models. The definitions of  $\theta_{i,j}$  and  $\theta_{jk}$  are sketched in the right-hand upper corner.

tum cutoff for the particles is raised from 0.1 to 0.5  $\text{GeV}/c$ . To verify that the model results are not significantly changed by the inclusion of "four-parton" events, the analysis was repeated taking only "four-parton" events [11], yielding a value of  $1.13 \pm 0.05$  for the ratio. Note that the "four-parton" events in our three-jet sample amount to at most 20%.

The increase of the effect with higher transverse

Table 1

The ratio of the particles emitted in the angular range  $0.3 < \theta_{i,j}/\theta_{jk} < 0.7$  between jets #1 and #2 together with the statistical errors, both for the data and the model calculations. The last line shows the corresponding ratio for the energy flow of both charged and neutral particles (see text for details).

particles		Data	Lund model	Hoyer model	
				$a_g = 4.0$	
				$\sigma_{q,g} = 500 \text{ MeV}$	$g = q$
ratio of number of particles	all	$1.39 \pm 0.04$	$1.33 \pm 0.03$	$1.09 \pm 0.03$	$1.03 \pm 0.03$
	charged only	$1.42 \pm 0.06$	$1.27 \pm 0.03$	$1.04 \pm 0.04$	$1.02 \pm 0.04$
	$p_{\perp}^{\text{out}} > 0.3 \text{ GeV}/c$	$1.73 \pm 0.13$	$1.55 \pm 0.07$	$1.12 \pm 0.07$	$0.96 \pm 0.07$
	$p_{\perp}^{\text{out}} \leq 0.3 \text{ GeV}/c$	$1.82 \pm 0.16$	$1.52 \pm 0.08$	$1.14 \pm 0.09$	$1.01 \pm 0.09$
	charged only				
	K	$1.9 \pm 0.2$	$1.7 \pm 0.15$	$1.14 \pm 0.1$	$1.0 \pm 0.1$
ratio of energy	all	$1.56 \pm 0.04$	$1.50 \pm 0.03$	$1.20 \pm 0.03$	$1.09 \pm 0.03$

mass is quantified in rows 3 and 4 of table 1, where the ratio is given for particles with  $p_{\perp}^{\text{out}} > 0.3 \text{ GeV}/c$  only. Increasing the transverse mass by only accepting K-meson candidates, yields similar results which are listed in row 5 of table 1. For  $p < 0.8 \text{ GeV}/c$ , these candidates are charged kaons identified by the measurement of their energy loss in the central detector [12] while for  $p > 0.8 \text{ GeV}/c$ , reconstructed neutral kaons [13] are used. The background of this enriched kaon sample is estimated to be about 50% for the data and the model calculations. The ratio of the energies flowing into these regions is given in row 6 of table 1.

Fragmentation along the colour-anticolour axes, however, provides a better description of the particle distributions not only in the angular gaps between jets #1 and #2 but also within the jets. Excluding for instance the range  $50^{\circ} < \theta < 120^{\circ}$  in the energy flow distribution (fig. 1a) from the comparison, one still obtains  $\chi^2/\text{dof} = 2 (5)$  of the Lund (Hoyer et al.) model. The following analysis suggested in ref. [14] shows that at least part of this difference is due to the different fragmentation schemes. For each particle in a jet,  $p_{\perp}^{\text{in}}$ , the momentum component in the  $(q_2, q_3)$ -plane transverse to the jet axis is calculated. The sign of  $p_{\perp}^{\text{in}}$  for each jet is defined by the insert in fig. 3a. Fig. 3 shows  $\langle p_{\perp}^{\text{in}} \rangle$  plotted as a function of  $p_{\parallel}$ , where  $p_{\parallel}$  is the momentum component parallel to the jet axis. In the figure, the point at  $p_{\parallel} = 5.5 \text{ GeV}/c$  includes all momenta above  $5.0 \text{ GeV}/c$ . Also shown are the predictions of the two models, whose statistical errors are less than half of those of the data. At very low values of  $p_{\parallel}$  the data and both models show a similar trend, in that  $\langle p_{\perp}^{\text{in}} \rangle$  points towards the neighbouring jet separated by the larger angular distance. For  $p_{\parallel} > 2.5 \text{ GeV}/c$ , however, the two model predictions diverge. For the data and the Lund model  $\langle p_{\perp}^{\text{in}} \rangle$  is positive (negative) for jet #1 (#2) and increases (decreases) with increasing  $p_{\parallel}$ . This effect is not only caused by the different particle densities in the gap between jets #1 and #2.

To show this, the particles in the region  $50^{\circ} < \theta < 120^{\circ}$  were excluded from the analysis and the jet axes were redetermined. The results show the same tendency as in fig. 3. A comparison of the data and of the model prediction for the restricted sample, taking the 4 points with  $p_{\parallel} > 2.5 \text{ GeV}/c$  yields  $\chi^2 = 13(10)$  for jet #1 (#2) in the case of the model of Hoyer et al. and

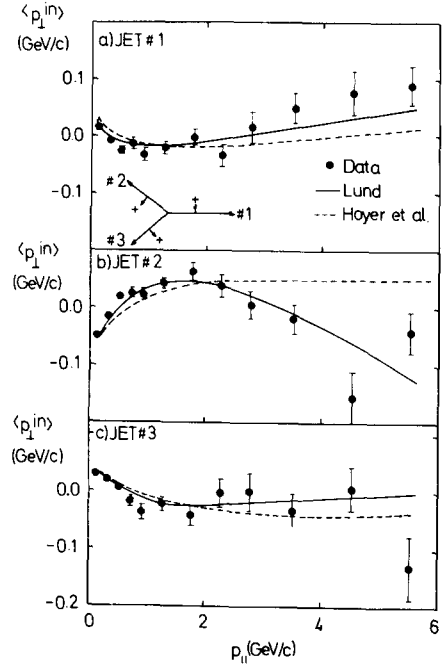


Fig. 3. The average momentum component in the  $(q_2, q_3)$ -plane transverse to the jet axis  $\langle p_{\perp}^{\text{in}} \rangle$  as a function of the momentum component parallel to the jet axis for the charged particles of jets #1, #2 and #3, respectively. The sign of  $p_{\perp}^{\text{in}}$  for each jet is defined by the insert in (a). The predictions of the model of Hoyer et al. and the Lund model are also shown.

$\chi^2 = 2 (4)$  in the case of the Lund model.

This effect is qualitatively and quantitatively understood in the colour string picture. The momentum vectors of the low momentum particles in the quark and antiquark jet, due to the above Lorentz transformation, are pulled towards the gluon direction, which for the majority of the events is the direction of jet #3. This results in a slightly larger opening angle between the  $q$  and  $\bar{q}$  jet than expected from independent parton fragmentation. Since the high momentum particles are less affected by the transformation, their average momenta tend to subtend a larger angle with jet axis #3 than the corresponding jet axes.

In summary, the measured energy and particle flow distributions of planar three-jet events, show a depletion in the angular gap between the two high energy jets relative to the gaps on both sides of the lowest energy jet. This becomes more pronounced as the transverse mass of the particles increases. The high momentum particles contained in each quark jet show

a net transverse momentum component in the event plane with respect to the jet axis, which points away from the gluon jet. The string model of the Lund group reproduces these observations while the model of Hoyer et al. fails to account for them, even in the fragmentation of the gluon is made considerably softer than that of quarks. The above phenomena support fragmentation along the colour flux lines.

We acknowledge the efforts of the PETRA machine group, who provided us with the opportunity of doing this experiment, and also the efforts of the technical support groups of the participating institutes in the construction and maintenance of our apparatus. This experiment was supported by the Bundesministerium für Forschung und Technologie, by the Education Ministry of Japan and by the U.K. Science and Engineering Research Council through the Rutherford Appleton Laboratory. The visiting groups at DESY wish to thank the DESY directorate for their hospitality.

#### References

- [1] JADE Collab., W. Bartel et al., Phys. Lett. 91 B (1980) 142;
- MARK J Collab., D.P. Barber et al., Phys. Rev. Lett. 43 (1979) 830;
- PLUTO Collab., Ch. Berger et al., Phys. Lett. 86B (1979) 418;
- TASSO Collab., R. Brandelik et al., Phys. Lett. 86B (1979) 243.
- [2] JADE Collab., W. Bartel et al., Phys. Lett. 115B (1982) 338.
- [3] JADE Collab., W. Bartel et al., Phys. Lett. 101B (1981) 129.
- [4] JADE Collab., W. Bartel et al., Phys. Lett. 88B (1979) 171
- [5] S. Brandt and H. Dahmen, Z. Phys. C1 (1979) 61; S.L. Wu and G. Zoernig, Z. Phys. C2 (1979) 107.
- [6] R.D. Field and R.P. Feynman, Nucl. Phys. B136 (1978) 1.
- [7] P. Hoyer, P. Osland, H.-G. Sander, T.F. Walsh, and P.M. Zerwas, Nucl. Phys. B161 (1979) 349.
- [8] JADE Collab., W. Bartel et al., Phys. Lett. 123B (1983) 460.
- [9] B. Andersson, G. Gustafson and C. Petersen, Z. Phys. C1 (1978) 105; B. Andersson and G. Gustafson, Z. Phys. C3 (1980) 223; B. Andersson, G. Gustafson and T. Sjöstrand, Z. Phys. C6 (1980) 235; Phys. Lett. 94B (1980) 211; T. Sjöstrand, Comput. Phys. Comm. 27 (1982) 243.
- [10] JADE Collab., W. Bartel et al., to be submitted to Z. Phys. C.
- [11] A. Ali, Phys. Lett. 110B (1982) 67.
- [12] JADE Collab., W. Bartel et al., Z. Phys. C6 (1980) 296.
- [13] JADE Collab., W. Bartel et al., DESY 83/042 (June 1983), to be published in Z. Phys. C.
- [14] T. Sjöstrand, private communication.